Received: 16 March 2018 | Accepted: 23 April 2018
DOI: 10.1002/jcb.27060

Check for updates

RESEARCH ARTICLE

WILEY Journal of Cellular Biochemistry

Effect of bone morphogenetic protein 9 on osteoblast differentiation of cells grown on titanium with nanotopography

Alann T.P. Souza | **Barbara L.S. Bezerra** | **Fabiola S. Oliveira** | **Gileade P. Freitas** | **Rayana L. Bighetti Trevisan** | **Paulo T. Oliveira** | **Adalberto L. Rosa** | **Marcio M. Beloti**

Cell Culture Laboratory, School of Dentistry of Ribeirão Preto, University of São Paulo, Ribeirão Preto, São Paulo, Brazil

Correspondence
Marcio M. Beloti, Cell Culture Laboratory, School of Dentistry of Ribeirão Preto, University of São Paulo, Av do Café s/n, 14040-904, Ribeirão Preto, SP, Brazil.
Email: mmbeloti@usp.br

Funding information
Fundação de Amparo à Pesquisa do Estado de São Paulo, Grant numbers: 2016/14477-1, 2016/14171-0

Abstract

Among bone morphogenetic proteins (BMPs), BMP-9 has been described as one with higher osteogenic potential. Here, we aimed at evaluating the effect of BMP-9 on the osteoblast differentiation of cells grown on titanium (Ti) with nanotopography, a well-known osseoinductive surface. MC3T3-E1 cells were grown either in absence or presence of BMP-9 (20 nM) on Ti with nanotopography (Ti-Nano) or machined Ti (Ti-Machined) for up to 21 days to evaluate the gene expression of RUNX2, osterix, osteocalcin, bone sialoprotein, SMAD6 and SMAD4, protein expression of SMAD4, ALP activity and extracellular matrix mineralization. As expected BMP-9 increased osteoblast differentiation irrespective of Ti surface topography; however, the cells grown on Ti-Nano were more responsible to BMP-9 compared with cells grown on Ti-machined. This could be, at least in part, due to the fact that Ti-Nano may act on both ways, by increasing the activation (SMAD4) and decreasing the inhibition (SMAD6) of the signaling pathway triggered by BMP-9, while Ti-Machined only decrease the inhibition (SMAD6) of this pathway. In conclusion, the combination of the osteogenic potential of BMP-9 with the osseoinductive capacity of Ti-Nano could be a promising strategy to favor the osseointegration of Ti implants.

KEYWORDS
bone, bone morphogenetic protein, nanotopography, osteoblast, titanium

1 | INTRODUCTION

In the last decades, several regulatory pathways involved in the osteoblast differentiation have been investigated.[1–5] Transcription factors, chromatin structure modifiers and signaling molecules such as bone morphogenetic proteins (BMPs) play a key role in this event.[6–8] BMPs are growth factors belonging to the transforming growth factor beta (TGF-β) family and some members are potent osseoinductive agents.[9–13]

The BMP canonical or SMAD-dependent signaling pathway is activated by the binding of a BMP to heterodimeric complexes of serine/threonine kinase receptors composed by type I and type II receptors.[10,14] Upon binding of BMP to the receptor complex, the SMAD1/5/8 phosphorylation occurs, which forms heterodimeric complexes with SMAD4 and the active complex is translocated to the nucleus and acts as a transcription factor inducing the expression of BMP target genes.[15,16] The SMAD1/5/8-SMAD4 signaling

 © 2018 Wiley Periodicals, Inc.

can be blocked by SMAD6, which prevents the translocation of the heterodimeric complex to the nucleus.[17]

Among the BMPs, the BMP-9 is still underexplored in terms of osteogenic potential. It has been shown that BMP-9 induces osteoblast differentiation of stem cells by activating the SMAD-dependent signaling pathway.[18,19] Additionally, in pre-osteoblastic cell line MC3T3-E1, BMP-9 exhibited higher osteogenic potential than BMP-2,[20,21] making BMP-9 an important target for therapies related to the bone tissue, including the osseointegration of titanium (Ti) implants.

The biocompatibility of implants is strongly affected by the interaction between osteoblasts and the biomaterial surface.[22,23] The Ti is the most frequently biomaterial used for implant manufacturing based on its excellent mechanical and biological properties. The proportion of direct contact between bone and Ti is influenced by clinical parameters and implant characteristics, such as chemistry and surface topography.[24] Considering the scale of topography, a Ti surface with nanotopography can be generated by a simple method, based on controlled deoxidation and reoxidation, using chemical conditioning with sulfuric acid/hydrogen peroxide (H_2SO_4/H_2O_2) solution.[25] It has been shown that this nanotopography is capable of inducing osteoblast differentiation, at least in part, through the modulation of BMP-2 signaling pathway.[26–31] However, up to now, to the best of our knowledge there are no data in the literature about the possible effect of BMP-9 on the interaction between osteoblasts and Ti and if this is modulated by surface topography. In this context, the aim of this study was to evaluate the effect of bone BMP-9 on osteoblast differentiation of cells grown on Ti with nanotopography compared with a machined Ti surface.

2 | MATERIALS AND METHODS

2.1 | Selection of BMP-9 concentration

MC3T3-E1 pre-osteoblastic cell line (subclone 14, American Type Culture Collection, Manassas, VA) was plated in 75 cm^2 flasks in growth medium that is alpha-minimum essential medium (α-MEM, Gibco, Grand Island, NY) supplemented with 10% fetal calf serum (Gibco), 50 mg/mL gentamicin (Gibco) and 0.3 mg/mL fungisone (Gibco) until subconfluence. After that, to select the more efficient concentration of BMP-9 in terms of osteogenic potential, cells were cultured in 24-well polystyrene plates (Corning Incorporated, Corning, New York, NY) at a density of 2×10^4 cells/well in osteogenic medium that is growth medium supplemented with 5 μg/mL ascorbic acid (Gibco-Invitrogen) and 7 mM β-glycerophosphate (Sigma-Aldrich, Darmstadt, Germany) for up to 7 days and exposed, during the final 24 h of the culture, to different concentrations of BMP-9. In the first set of experiments, we used 0 nM-vehicle (Control), 0.1, 1, and 100 nM and in the second, Control, 10, 20, and 40 nM. At Day 7, the gene expression of two osteoblast markers, runt-related transcription factor 2 (RUNX2) and alkaline phosphatase (ALP) was evaluated by real-time PCR as described below. All cell cultures were kept at 37°C in a humidified atmosphere of 5% CO_2 and 95% air and the culture medium was changed every 2-3 days.

2.2 | Gene expression of RUNX2 and ALP

Quantitative real-time PCR was carried out at Day 7 to evaluate the gene expression of RUNX2 and ALP. The total RNA was extracted with Trizol reagent (Invitrogen, Carlsbad, CA) according to the manufacturer's instructions. To synthesize complementary DNA (cDNA) through a reverse transcription reaction (M-MLV reverse transcriptase, Promega Corporation, Madison, WI) we used 1 μg of RNA. The reactions were carried out ($n = 4$) in the Step One Plus Real-Time PCR System (Invitrogen) using Taqman PCR Master Mix (Applied Biosystems, Foster City, CA). The relative gene expression was normalized to β-actin expression and the real changes were expressed relative to the gene expression of the Control cultures using the comparative threshold method ($2^{-\Delta\Delta Ct}$).[32]

2.3 | Preparation of Ti surfaces

Discs of commercially pure grade 2 Ti, with 12 mm in diameter and 1.5 mm thick, were polished using 320 and 600 grit silicon carbide, cleaned by sonication and rinsed with toluene. Samples were treated with a blend of 10 N H_2SO_4 and 30% aqueous H_2O_2 (1:1 v/v) for 4 h at room temperature under continuous agitation to produce the surface with nanotopography.[25] Treated (Ti-Nano) and untreated (Ti-Machined) discs were rinsed with deionized H_2O several times, autoclaved and air-dried. The surfaces were examined using a field emission scanning electron microscope operated at 5 kV (Inspect S50, FEI, Hillsboro, OR).

2.4 | Effect of BMP-9 on cells grown on Ti surfaces

MC3T3-E1 cells were cultured in growth medium until subconfluence as described above. Then, cells were plated on Ti-Nano or Ti-Machined discs in 24-well culture plates (Corning Incorporated) at a density of 2×10^4 cells/disc in osteogenic medium containing BMP-9 in the previously selected concentration for periods of up to 21 days to evaluate the parameters described below. All cell cultures were kept at 37°C in a humidified atmosphere of 5% CO_2 and 95% air and the culture medium was changed every 2-3 days.

2.5 | Gene expression of osteoblast markers and SMADs

At Day 7, quantitative real-time PCR was carried out as described above to evaluate the gene expression of the osteoblast markers, RUNX2, osterix (OSX), osteocalcin (OC), and bone sialoprotein (BSP), in addition to SMAD4 and SMAD6. The relative gene expression ($n = 3$) was normalized to β-actin expression and the real changes were expressed relative to cells grown on either Ti-Nano or Ti-Machined surfaces in the absence of BMP-9 (Control) using the comparative threshold method ($2^{-\Delta\Delta Ct}$).[32]

2.6 | SMAD4 protein detection

At Day 7, the SMAD4 protein was detected by Western blotting. Cells grown on Ti-Nano or Ti-Machined, with or without exogenous BMP-9, were lysed in 140 μL of RIPA buffer containing 1 × protease inhibitor mixture (Roche Applied Science, Indianapolis, IN), 1 mM phenylmethanesulfonyl fluoride (Sigma-Aldrich) and 25 μM MG132 proteasome inhibitor (Roche Applied Science) and boiled for 5 min. Briefly, 80 μg of total protein of each sample was subjected to electrophoresis in a denaturing 10% polyacrylamide gel and transferred to a Hybond C-Extra membrane (GE Healthcare Life Science, Piscataway, NJ) using a semidry transfer apparatus (Bio-Rad Laboratories, Hercules, CA). The membrane was blocked for 2 h in Tris-buffered saline plus 0.1% Tween 20 (TBS-T; Sigma-Aldrich) containing 5% bovine serum albumin (BSA; Sigma-Aldrich). The SMAD4 protein was detected by incubating the membrane using rabbit polyclonal antibody to SMAD4 (1:1,000, Santa Cruz Biotechnology, Santa Cruz, CA) overnight at 4°C, followed by secondary antibody, goat anti-rabbit IgG-horseradish peroxidase (HRP) conjugate (1:2,000, Santa Cruz Biotechnology) for 1 h at room temperature. Mouse monoclonal anti-glyceraldehyde-3-phosphate dehydrogenase (GAPDH) (1:2,000, Santa Cruz Biotechnology) was used as a control followed by the secondary antibody, goat anti-mouse IgG-HRP conjugate (1:3,000, Santa Cruz Biotechnology). The secondary antibodies were detected using Western Lightning Chemiluminescence Reagent (PerkinElmer Life Sciences, Waltham, MA) and the images were acquired using G:Box gel imaging (Syngene, Cambridge, UK). The SMAD4 expression was quantified by counting pixels and normalized to the expression of GAPDH.

2.7 | ALP activity

On Day 10, the release of thymolphthalein from the hydrolysis of thymolphthalein monophosphate substrate was used to indirectly detect the ALP activity in cells grown on Ti-Nano or Ti-Machined surfaces, with or without exogenous BMP-9, using a commercial kit (Labtest Diagnostica, Lagoa Santa, MG, Brazil). Briefly, to obtain the cell lysates, 1 mL of 0.1% sodium lauryl sulfate solution (Sigma-Aldrich) was added to each well containing the Ti discs and after 30 min, 50 μL of thymolphthalein monophosphate was mixed with 0.5 mL of 0.3 M diethanolamine buffer, pH 10.1, and left for 2 min at 37°C. Then, 50 μL of the cell lysates from each Ti disc were added, and after 10 min at 37°C, 2 mL of a solution of Na_2CO_3 (0.09 mmol/mL) and NaOH (0.25 mmol/mL) were used to stop the reaction. The absorbance was measured at 590 nm in the plate reader μQuant (Bio-Tek Instruments Inc., Winooski, VT) in quintuplicate ($n = 5$) and ALP activity was calculated from a thymolphthalein standard curve and normalized to the amount of total protein. The ALP activity was expressed as μmol of thymolphthalein/h/mg protein.

2.8 | Extracellular matrix mineralization

On Day 21, cells grown on Ti-Nano or Ti-Machined surfaces, with or without exogenous BMP-9, were fixed in 10% formalin for 2 h at room temperature, dehydrated and stained with 2% Alizarin red S (Sigma-Aldrich), pH 4.2, for 10 min. Images were captured with a high-resolution digital camera (Canon EOS Digital Rebel Camera, Canon, Lake Success, NY) for qualitative analysis. The calcium content was measured using a colorimetric method. Briefly, 280 μL of 10% acetic acid were added to each well containing the Ti discs and incubated at room temperature for 30 min under shaking at 400 rpm. This solution was vortexed for 1 min, heated to 85°C for 10 min, and transferred to ice for 5 min. The slurry was centrifuged at 13 000*g* for 15 min and 100 μL of the supernatant was mixed with 40 μL of 10% ammonium hydroxide. The absorbance was read at 405 nm ($n = 5$) in the plate reader μQuant (Bio-Tek Instruments Inc.) and the data were expressed as absorbance.

2.9 | Statistical analysis

The data of the gene expression used to select the BMP-9 concentration were analyzed by one-way ANOVA, followed by Student-Newman-Keuls when applied. The data of the experiments to evaluated the effect of BMP-9 on cells grown on either Ti-Nano or Ti-Machined were analyzed by Student's *t*-test. The level of significance was set at 5% ($P \leq 0.05$).

3 | RESULTS

3.1 | Selection of BMP-9 concentration

In the first set of experiments, the gene expression of RUNX2 (Figure 1A) and ALP (Figure 1B) was higher using 10 nM of

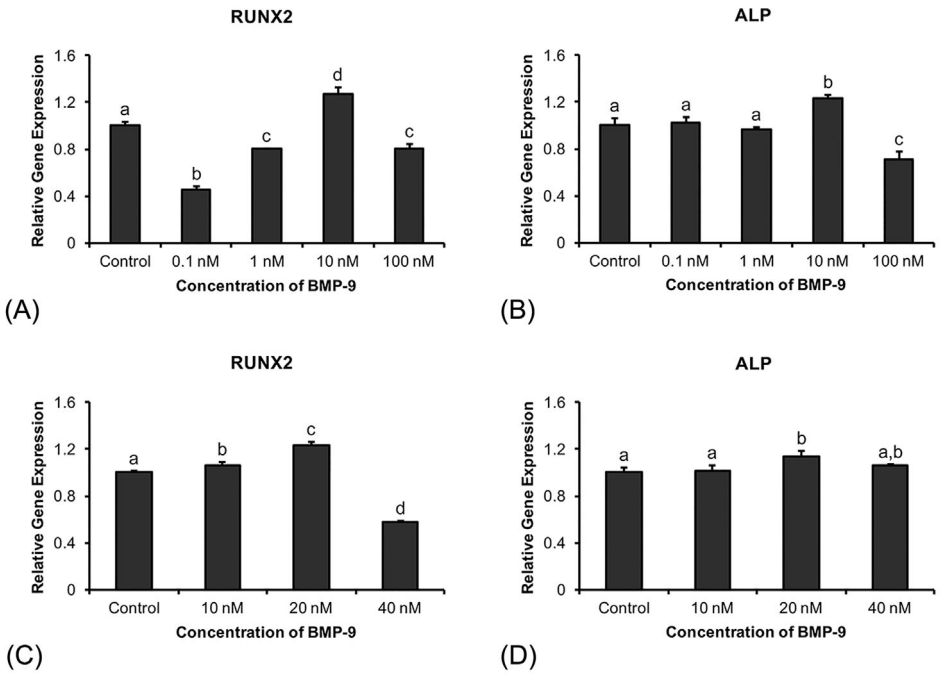

FIGURE 1 Gene expression of RUNX2 (A and C) and ALP (B and D) in MC3T3-E1 cells grown on polystyrene for 7 days and exposed to different concentrations of BMP-9 in the last 24 h of culture. The data presented are mean ± standard deviation ($n = 4$) and different letters indicate a statistically significant difference ($P \leq 0.05$)

BMP-9 compared with the Control and all other concentrations we have tested ($P = 0.001$ for both RUNX2 and ALP, and all BMP-9 concentrations). These results indicated that, among the tested concentrations of BMP-9, 10 nM of BMP-9 exhibited the higher osteogenic potential. However, due to the large gap between the two highest concentrations (10 and 100 nM) an additional set of experiments was done using two additional concentrations of BMP-9 (20 and 40 nM) to be compared with the Control and the 10 nM. In this scenario, the gene expression of RUNX2 (Figure 1C) was higher using 20 nM of BMP-9, compared with 10 nM, 40 nM ($P = 0.001$ for both) and Control ($P = 0.033$). Similarly, the gene expression of ALP (Figure 1D) was higher using 20 nM compared with 10 nM and Control ($P = 0.001$ for both), while no statistically significant difference was detected between 20 and 40 nM ($P = 0.187$). Taken together, the results indicated that, among the tested concentrations of BMP-9, 20 nM exhibited the higher osteogenic potential and therefore, this was the concentration selected to evaluate the effect of BMP-9 on cells grown on Ti-Nano and Ti-Machined.

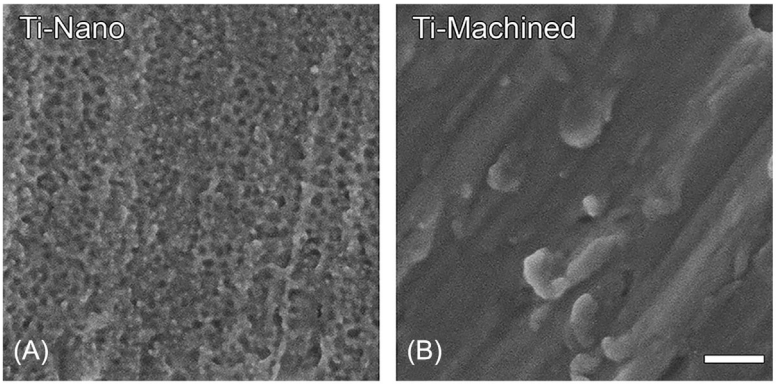

FIGURE 2 High-resolution scanning electron micrographs of Ti-Nano (A) and Ti-Machined (B). Ti-Nano exhibits a network of nanopores while Ti-Machined presents a smooth surface. Scale bar (A and B): 100 nm

3.2 | Ti surfaces

Under scanning electron microscopy, the Ti-Nano and Ti-Machined exhibited remarkable differences in terms of surface topography. The Ti-Nano (Figure 2A), as expected, exhibited a network of nanopores, indicating that the treatment with H_2SO_4/H_2O_2 was efficient to generate the nanotopography, while Ti-Machined (Figure 2B) showed a smoother surface.

3.3 | Effect of BMP-9 on osteoblast differentiation of cells grown on Ti surfaces

In general, BMP-9 increased the gene expression of the osteoblast markers in cells grown on Ti-Nano, but not on Ti-Machined. The BMP-9 increased the gene expression of RUNX2 ($P = 0.001$), OSX ($P = 0.018$), OC ($P = 0.001$), and BSP ($P = 0.003$) in cells grown on Ti-Nano (Figure 3A). In cells grown on Ti-Machined, the BMP-9 increased the gene expression of OSX ($P = 0.005$), decreased OC ($P = 0.021$) and did not affect RUNX2 ($P = 1.000$) and BSP ($P = 0.155$) (Figure 3B). The BMP-9 reduced the gene expression of SMAD6 in cells grown on both Ti-Nano ($P = 0.002$) (Figure 4A) and Ti-Machined ($P = 0.046$) (Figure 4C). Furthermore, BMP-9 increased the gene expression of SMAD4 in cells grown on Ti-Nano ($P = 0.019$) (Figure 4A), while no effect was observed in cells grown on Ti-Machined ($P = 0.114$) (Figure 4C).

Corroborating the gene expression findings, BMP-9 increased the SMAD4 protein expression in cells grown on Ti-Nano (1.6-fold) (Figure 4B) and slightly decreased its expression in cells grown on Ti-Machined (1.1-fold) (Figure 4D).

The BMP-9 increased the ALP activity in cells grown on Ti-Nano ($P = 0.027$) (Figure 5A), without affecting its activity in cells grown on Ti-Machined ($P = 0.758$) (Figure 5C).

The extracellular matrix mineralization was increased in the presence of BMP-9 in cultures grown on both Ti-Nano ($P = 0.008$) (Figure 5B) and Ti-Machined ($P = 0.032$) (Figure 5D).

4 | DISCUSSION

This study aimed to evaluate the effect of BMP-9 on osteoblast differentiation induced by Ti with nanotopography. Based on dose-response experiments, we selected the concentration of 20 nM of BMP-9 as being the most effective in MC3T3-E1 cells and further use in cultures grown on either Ti-Nano or Ti-Machined. The results showed that, in general, BMP-9 regulates the interaction between cells and Ti irrespective of surface topography; however, the cells grown on Ti-Nano were more responsive to BMP-9 in terms of osteoblast differentiation.

For this study BMP-9 was chosen due to its higher osteogenic potential compared with other BMPs, such as BMP-2, -4, and -7.[33,34] Considering that osteoblasts express some BMPs with osseoinductive capacity like BMP-2, -4 and -7,[35–37] we evaluated the expression of endogenous BMP-9 in both MC3T3-E1 cells and osteoblasts differentiated from bone marrow mesenchymal stem cells in order to investigate

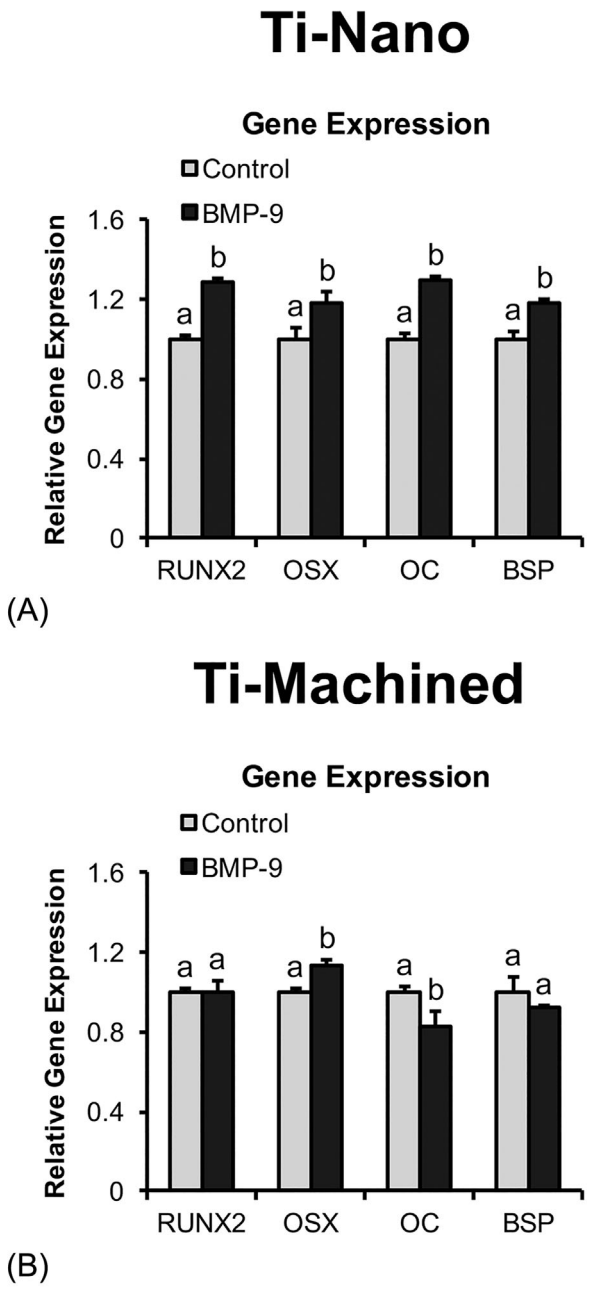

FIGURE 3 Gene expression of the osteoblast markers RUNX2, OSX, OC, BSP in MC3T3-E1 cells grown on Ti-Nano (A) or Ti-Machined (B) and treated with 20 nM of BMP-9 or vehicle (Control) on Day 7. The data presented are mean ± standard deviation ($n = 3$) and different letters indicate a statistically significant difference between Control and BMP-9 for each evaluated gene ($P \leq 0.05$)

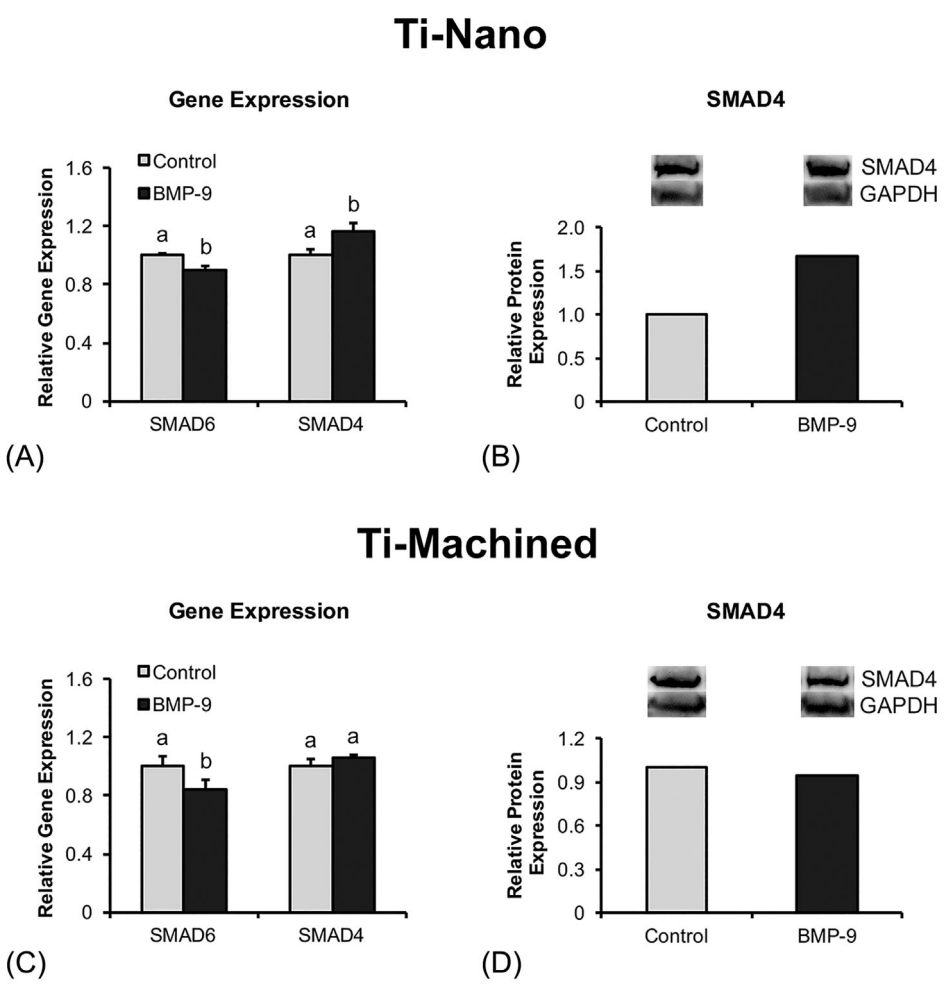

FIGURE 4 Gene expression of the SMAD family proteins SMAD6 and SMAD4 (A and C) and protein expression of SMAD4 (B and D) in MC3T3-E1 cells grown on Ti-Nano (A and B) or Ti-Machined (C and D) and treated with 20 nM of BMP-9 or vehicle (Control) on Day 7. The data presented are mean ± standard deviation ($n = 3$) and different letters indicate a statistically significant difference between Control and BMP-9 for each evaluated gene ($P \leq 0.05$)

its role in osteoblast differentiation induced by Ti-Nano. However, BMP-9 gene expression was not detected in these cells, unlike organs and tissues where this protein is known to be expressed (Figure S1),[38,39] suggesting that despite the relevance of BMP-9 to osteoblast differentiation, this protein is not synthesized by bone tissue.

The concentrations tested to select the amount of exogenous BMP-9 were based on a study developed with the same protein and cell type used here,[21] but while those authors evaluated the ability of BMP-9 in activating BMP and MAPK signaling pathways, here the concentration of BMP-9 was selected based on its potential to increase RUNX2 and ALP gene expression. These genes were selected as RUNX2 is an essential transcription factor and the master regulator of osteoblast differentiation and ALP is essential for bone mineralization.[40–42] Following a short exposure time, the concentration of 20 nM of BMP-9 increased the gene expression of both RUNX2 and ALP and, therefore, this concentration was used to evaluate the effect of BMP-9 in cells grown on either Ti-Nano or Ti-Machined.

It is well documented that nanotopography affects mechanisms involved in the osteoblast differentiation.[27,28,43] Previously, our research group showed that Ti-Nano induces osteoblast differentiation by at least two major pathways, increasing the expression of α1β1 integrin and modulating integrin signaling pathway and up-regulating the BMP signaling pathway by a combination of increasing endogenous production of BMP-2 and down-regulating the expression of microRNA-4448, -4708 and -4773, which inhibit SMAD1 and SMAD4, both transducers of BMP-2 osteogenic signal.[28,29,43] Additionally, it was demonstrated that cells grown on Ti-Nano are more responsive to BMP-2 than cells grown on Ti-Machined.[28] In keeping with this, this study showed that MC3T3-E1 cells grown on Ti-Nano are also

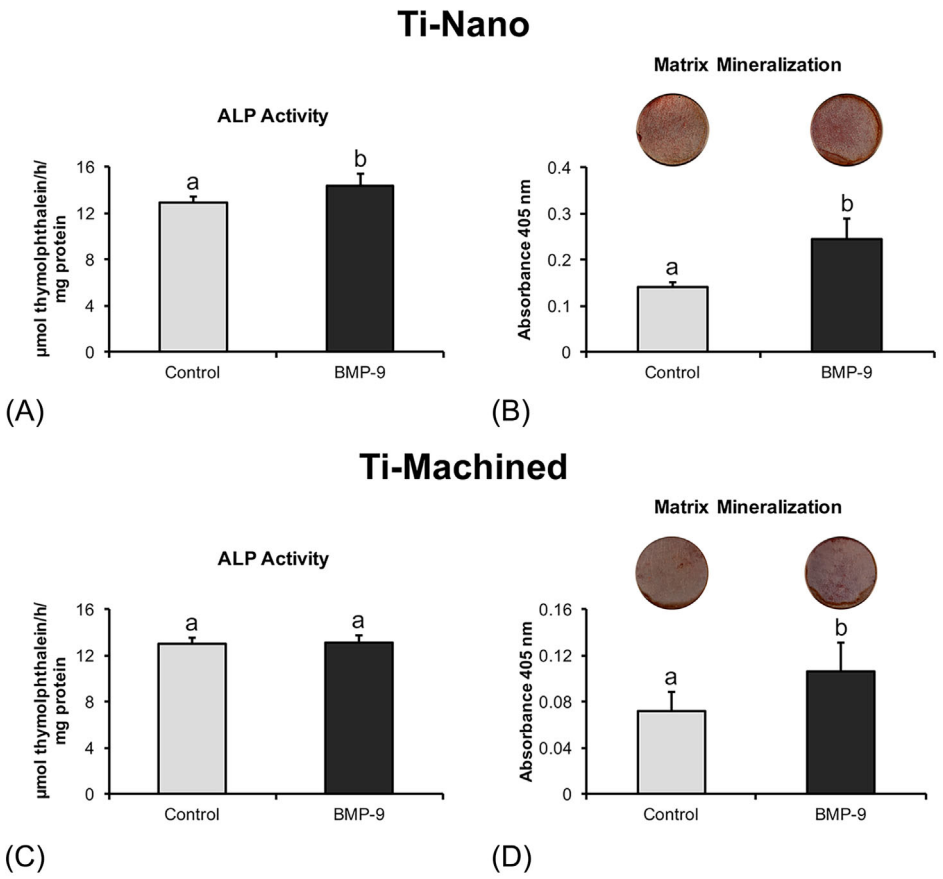

FIGURE 5 ALP activity (A and C) on Day 10 and extracellular matrix mineralization (B and D) on Day 21 in MC3T3-E1 cells grown on Ti-Nano (A and B) or Ti-Machined (C and D) and treated with 20 nM of BMP-9 or vehicle (Control). The data presented are mean ± standard deviation ($n = 5$) and different letters indicate a statistically significant difference between Control and BMP-9 for each evaluated parameter ($P \leq 0.05$)

more responsive to BMP-9 compared with those grown on Ti-Machined. The BMP-9 induced higher expression of the osteoblast markers RUNX2, OSX, OC, and BSP and increased ALP activity and extracellular matrix mineralization in cultures grown on Ti-Nano, while in cultures grown on Ti-Machined, BMP-9 only increased OSX gene expression and extracellular matrix mineralization. Corroborating these findings, it was demonstrated that BMP-9 upregulates osteoblast differentiation-related genes in mesenchymal stem cells.[44]

As the action of BMPs depends on a cascade of signaling, including the participation of SMADs, we evaluated the expression of SMAD6 and SMAD4 in cells grown on Ti-Nano and Ti-Machined in the presence of BMP-9. SMAD6 is an intracellular antagonist of the BMP signaling and SMAD4 is a common mediator SMAD, essential to the activation of BMP pathway.[45] The higher gene and protein expression of SMAD4 and the lower SMAD6 gene expression induced by BMP-9 in cells grown on Ti-Nano suggest that Ti-Nano acts on both sides, increasing the activation and decreasing the inhibition of the signaling pathway triggered by BMP-9. On the other hand, in cells grown on Ti-Machined, BMP-9 only reduced the expression of SMAD6, suggesting that Ti-Machined acts only by decreasing the inhibition of the BMP-9 signaling pathway.

In conclusion, our results have shown that BMP-9 enhances the osteoblast differentiation of cells grown on Ti irrespective of surface topography. However, the cells grown on Ti-Nano were more responsive to BMP-9 in terms of osteoblast differentiation compared with cells grown on Ti-Machined. This could be, at least in part, because Ti-Nano may act on both ways, by increasing the activation and decreasing the inhibition of the signaling pathway triggered by BMP-9, while Ti-Machined only decreases the inhibition of this pathway. In this context, this study may contribute to understand the role of surface topography in the effects of BMPs on the interaction between bone tissue and Ti implants and, consequently, to the development of new strategies to favor the events related to the osseointegration process.

ACKNOWLEDGMENTS

Milla Sprone Tavares and Roger Rodrigo Fernandes are acknowledged for technical assistance during the experiments. State of São Paulo Research Foundation (FAPESP, Brazil); Grant number: # 2016/14477-1 and #2016/14171-0.

DISCLOSURES

All authors confirm that there is no conflict of interest associated with this study and there has been no financial support that could have influenced our outcomes.

ORCID

Marcio M. Beloti http://orcid.org/0000-0003-0149-7189

REFERENCES

1. Lindsley HB, Smith DD. Enhanced prostaglandin E2 secretion by cytokine-stimulated human synoviocytes in the presence of subtherapeutic concentrations of nonsteroidal antiinflammatory drugs. *Arthritis Rheum*. 1990;33:1162–1169.
2. Canalis E. Growth factor control of bone mass. *J Cell Biochem*. 2009;108:769–777.
3. Milat F, Ng KW. Is Wnt signalling the final common pathway leading to bone formation? *Mol Cell Endocrinol*. 2009;310:52–62.
4. Rosen V. BMP2 signaling in bone development and repair. *Cytokine Growth Factor Rev*. 2009;20:475–480.
5. Komori T. Regulation of bone development and extracellular matrix protein genes by RUNX2. *Cell Tissue Res*. 2010;339:189–195.
6. Lian JB, Stein GS, Javed A, et al. Networks and hubs for the transcriptional control of osteoblastogenesis. *Rev Endocr Metab Disord*. 2006;7:1–16.
7. Jensen ED, Nair AK, Westendorf JJ. Histone deacetylase co-repressor complex control of Runx2 and bone formation. *Crit Rev Eukaryot Gene Expr*. 2007;17:187–196.
8. Stein GS, Zaidi SK, Stein JL, et al. Transcription-factor-mediated epigenetic control of cell fate and lineage commitment. *Biochem Cell Biol*. 2009;87:1–6.
9. Haasemann M, Nawratil P, Muller-Esterl W. Rat tyrosine kinase inhibitor shows sequence similarity to human alpha 2-HS glycoprotein and bovine fetuin. *Biochem J*. 1991;274:899–902.
10. Senta H, Park H, Bergeron E, et al. Cell responses to bone morphogenetic proteins and peptides derived from them: biomedical applications and limitations. *Cytokine Growth Factor Rev*. 2009;20:213–222.
11. Singhatanadgit W, Olsen I. Endogenous BMPR-IB signaling is required for early osteoblast differentiation of human bone cells. *In Vitro Cell Dev Biol Anim*. 2011;47:251–259.
12. Bonilla-Claudio M, Wang J, Bai Y, Klysik E, Selever J, Martin JF. Bmp signaling regulates a dose-dependent transcriptional program to control facial skeletal development. *Development*. 2012;139:709–719.
13. Xiang L, Liang C, Zhen-Yong K, Liang-Jun Y, Zhong-Liang D. BMP9-induced osteogenetic differentiation and bone formation of muscle-derived stem cells. *J Biomed Biotechnol*. 2012;2012:610952.
14. Lavery K, Swain P, Falb D, Alaoui-Ismaili MH. BMP-2/4 and BMP-6/7 differentially utilize cell surface receptors to induce osteoblastic differentiation of human bone marrow-derived mesenchymal stem cells. *J Biol Chem*. 2008;283:20948–20958.
15. Miyazono K. Signal transduction by bone morphogenetic protein receptors: functional roles of Smad proteins. *Bone*. 1999;25:91–93.
16. Gazzerro E, Canalis E. Bone morphogenetic proteins and their antagonists. *Rev Endocr Metab Disord*. 2006;7:51–65.
17. Heliotis M, Tsiridis E. Suppression of bone morphogenetic protein inhibitors promotes osteogenic differentiation: therapeutic implications. *Arthritis Res Ther*. 2008;10:115.
18. Beederman M, Lamplot JD, Nan G, et al. BMP signaling in mesenchymal stem cell differentiation and bone formation. *J Biomed Sci Eng*. 2013;6:32–52.
19. Lamplot JD, Qin J, Nan G, et al. BMP9 signaling in stem cell differentiation and osteogenesis. *Am J Stem Cells*. 2013;2:1–21.
20. Bergeron E, Senta H, Mailloux A, Park H, Lord E, Faucheux N. Murine preosteoblast differentiation induced by a peptide derived from bone morphogenetic proteins-9. *Tissue Eng Part A*. 2009;15:3341–3349.
21. Lauzon MA, Daviau A, Drevelle O, Marcos B, Faucheux N. Identification of a growth factor mimicking the synergistic effect of fetal bovine serum on BMP-9 cell response. *Tissue Eng Part A*. 2014;20:2524–2535.
22. Brama M, Rhodes N, Hunt J, et al. Effect of titanium carbide coating on the osseointegration response in vitro and in vivo. *Biomaterials*. 2007;28:595–608.
23. Saranya N, Saravanan S, Moorthi A, Ramyakrishna B, Selvamurugan N. Enhanced osteoblast adhesion on polymeric nano-scaffolds for bone tissue engineering. *J Biomed Nanotechnol*. 2011;7:238–244.
24. Albrektsson T, Johansson J. Quantified bone tissue reactions to various metallic materials with reference to the so-called osseointegration concept. In: Davies JE, Albrektsson T, editors. *The Bone Biomaterial Interface*. Toronto: University of Toronto Press; 1991:357–363.
25. Nanci A, Wuest JD, Peru L, et al. Chemical modification of titanium surfaces for covalent attachment of biological molecules. *J Biomed Mater Res*. 1998;40:324–335.
26. de Oliveira PT, Nanci A. Nanotexturing of titanium-based surfaces upregulates expression of bone sialoprotein and osteopontin by cultured osteogenic cells. *Biomaterials*. 2004;25:403–413.
27. de Oliveira PT, Zalzal SF, Beloti MM, Rosa AL, Nanci A. Enhancement of in vitro osteogenesis on titanium by chemically produced nanotopography. *J Biomed Mater Res A*. 2007;80:554–564.
28. Kato RB, Roy B, De Oliveira FS, et al. Nanotopography directs mesenchymal stem cells to osteoblast lineage through regulation of microRNA-SMAD-BMP-2 circuit. *J Cell Physiol*. 2014;229:1690–1696.
29. Castro-Raucci LMS, Francischini MS, Teixeira LN, et al. Titanium with nanotopography induces osteoblast differentiation by regulating endogenous bone morphogenetic protein expression and signaling pathway. *J Cell Biochem*. 2016;117:1718–1726.
30. Lotz EM, Olivares-Navarrete R, Berner S, Boyan BD, Schwartz Z. Osteogenic response of human MSCs and osteoblasts to hydrophilic and hydrophobic nanostructured titanium implant surfaces. *J Biomed Mater Res A*. 2016;104:3137–3148.
31. Gulati K, Prideaux M, Kogawa M, et al. Anodized 3D-printed titanium implants with dual micro- and nano-scale topography

promote interaction with human osteoblasts and osteocyte-like cells. *J Tissue Eng Regen Med*. 2017;11:3313–3325.
32. Livak KJ, Schmittgen TD. Analysis of relative gene expression data using real-time quantitative PCR and the 2(-Delta Delta C(T)) Method. *Methods*. 2001;25:402–408.
33. Cheng H, Jiang W, Phillips FM, et al. Osteogenic activity of the fourteen types of human bone morphogenetic proteins (BMPs). *J Bone Joint Surg Am*. 2003;85-A:1544–1552.
34. Kang Q, Sun MH, Cheng H, et al. Characterization of the distinct orthotopic bone-forming activity of 14 BMPs using recombinant adenovirus-mediated gene delivery. *Gene Ther*. 2004;11:1312–1320.
35. Kureel J, Dixit M, Tyagi AM, et al. MiR-542-3p suppresses osteoblast cell proliferation and differentiation, targets BMP-7 signaling and inhibits bone formation. *Cell Death Dis*. 2014;5: e1050.
36. Velazquez-Cayon R, Castillo-Dali G, Corcuera-Flores JR, et al. Production of bone mineral material and BMP-2 in osteoblasts cultured on double acid-etched titanium. *Med Oral Patol Oral Cir Bucal*. 2017;22:e651–e659.
37. Hirai T. Regulation of clock genes by adrenergic receptor signaling in osteoblasts. *Neurochem Res*. 2018;43:120–126.
38. Miller AF, Harvey SA, Thies RS, Olson MS. Bone morphogenetic protein-9. An autocrine/paracrine cytokine in the liver. *J Biol Chem*. 2000;275:17937–17945.
39. Mellott TJ, Pender SM, Burke RM, Langley EA, Blusztajn JK. IGF2 ameliorates amyloidosis, increases cholinergic marker expression and raises BMP9 and neurotrophin levels in the hippocampus of the APPswePS1dE9 Alzheimer's disease model mice. *PLoS ONE*. 2014;9:e94287.
40. Millan JL. The role of phosphatases in the initiation of skeletal mineralization. *Calcif Tissue Int*. 2013;93:299–306.
41. Bover J, Urena P, Aguilar A, et al. Alkaline phosphatases in the complex chronic kidney disease-mineral and bone disorders. *Calcif Tissue Int*. 2018; https://doi.org/10.1007/s00223-018-0399-z
42. Komori T. Runx2, an inducer of osteoblast and chondrocyte differentiation. *Histochem Cell Biol*. 2018;149:313–323.
43. Rosa AL, Kato RB, Castro Raucci LM, et al. Nanotopography drives stem cell fate toward osteoblast differentiation through alpha1beta1 integrin signaling pathway. *J Cell Biochem*. 2014;115: 540–548.
44. Zhang W, Zhang L, Zhou Y, et al. Synergistic effects of BMP9 and miR-548d-5p on promoting osteogenic differentiation of mesenchymal stem cells. *Biomed Res Int*. 2015;2015:309747.
45. Carreira AC, Lojudice FH, Halcsik E, Navarro RD, Sogayar MC, Granjeiro JM. Bone morphogenetic proteins: facts, challenges, and future perspectives. *J Dent Res*. 2014;93:335–345.

SUPPORTING INFORMATION

Additional supporting information may be found online in the Supporting Information section at the end of the article.

How to cite this article: Souza ATP, Bezerra BLS, Oliveira FS, et al. Effect of bone morphogenetic protein 9 on osteoblast differentiation of cells grown on titanium with nanotopography. *J Cell Biochem*. 2018;1–9. https://doi.org/10.1002/jcb.27060